Enhancing the Electroluminescence Performances of Blue Polymer Light Emitting Devices Via Carriers Transporting Materials Incorporation

Rong-Ho Lee,[1] Hsin-Fang Hsu,[1] Li-Hsin Chan,[2] Chin-Ti Chen[2]

[1]*Department of Chemical and Material Engineering, National Yunlin University of Science and Technology, Yunlin 640, Taiwan, Republic of China*
[2]*Institute of Chemistry, Academia Sinica, Taipei, Taiwan 11529, Republic of China*

Received 20 July 2007; accepted 29 February 2008
DOI 10.1002/app.28384
Published online 9 May 2008 in Wiley InterScience (www.interscience.wiley.com).

ABSTRACT: A series of polymer light emitting devices (PLEDs) based on the composite films of *N*-arylbenzimidazoles trimer (TPBI), poly (*n*-vinylcarbazole) (PVK), and a triarylaminooxadiazole-containing tetraphenylsilane light emitting polymer (PTOA) were investigated. Electroluminescence (EL) performance is enhanced with doped TPBI into the light-emitting layer for the PTOA-based devices. A deep blue emission (Commission Internationale de L'Eclairage ($CIE_{x,y}$) corodinates (0.16,0.06)) is obtained for the TPBI-PTOA-based device. Brightness and current efficiency of the TPBI-PTOA-based device can be as high as 961 cd/m^2 and 1.85 cd/A, respectively. The EL performances of TPBI-PTOA composite film-based devices are further enhanced by inserting a TPBI layer into the light emitting layer and cathode interface for a better electron and hole charge balance. Doping TPBI into the light-emitting layer of PVK-PTOA is not favorable for enhanced EL performances. Brightness and current efficiency reduced with increasing TPBI content for the TPBI-PVK-PTOA-based devices. Similar results are obtained for devices based on the TPBI-PVK-PTOA/TPBI bi-layer composite solid film. Morphology and charge balance effects on EL performances of TPBI-PTOA and TPBI-PVK-PTOA composite films based PLEDs are discussed in detail. © 2008 Wiley Periodicals, Inc. J Appl Polym Sci 109: 2605–2615, 2008

Key words: light emitting polymer; carriers transporting material; electroluminesuence

INTRODUCTION

Polymer light emitting displays (PLEDs) have recently undergone extensive study, and appear ready for commercialization in the flat-panel display market, due to low turn on voltage, high brightness, high efficiency, easy processing, and low cost fabrication.[1,2] Electroluminescence (EL) performance of PLED is determined by intrinsic property of light emitting polymer (LEP),[3,4] device processing parameters,[5–11] and device configuration.[12] Charge balance throughout the device plays a key role for fabricating PLEDs with excellent EL properties, such as high brightness, high efficiency, and high operation stability.[13–32]

Adopting various strategies achieves a charge balance throughout the device resulting in PLED with excellent EL performance.[13–31] Inorganic thin film and a charge-transporting layer are typically inserted between a polymer light-emitting layer and electrode interface to create a reduced energy barrier for balanced charge injection.[13–21] The LiF insulating thin layer shows dramatic improvement of PLED quantum efficiency and lifetime due to better electron and hole current balance.[13–16] The hole-transporting layer on the other hand, is usually inserted between the anode and polymer light-emitting layer for reducing turn-on voltage, and enhancing operational stability of PLEDs.[17–19] Moreover, electron-transporting layer insertion between the polymer emitting layer and cathode also improves EL performances.[20,21] Both electron and hole transporting molecules are often incorporated into the polymer backbone of LEP.[22–29] For example, oxadiazole-containing compounds with electron-withdrawing properties are usually incorporated into the blue LEP backbone.[22–27] Introducing the oxadiazole group could enhance blue LEP electron affinity, causing energy barrier reduction between the light emitting layer and metal cathode.[22–27] The aromatic amine-containing compound is typically grafted into the polymer backbone for LEP hole transporting property enhancement.[28,29] Single-layer PLEDs with polymer blends of conjugated polymer and electron or hole carrier transporting materials have alternatively been investigated.[30–35] Enhanced brightness of blue LEPs by blending with hole-transporting materials (HTM) has been reported by Suh et al.[30] PLEDs

Correspondence to: R. Lee (lerongho@yuntech.edu.tw).
Contract grant sponsor: National Science Council of Taiwan, ROC; contract grant number: NSC 95-2221-E-224-046.

containing a blend of MEH-PPV and an electron-transporting material (ETM) have also been fabricated.[31,32] The EL performances of PLEDs increase significantly over obtained devices based only on MEH-PPV. Efficient single-layer polymer phosphorescent light-emitting devices based on the iridium complex and a hole-transporting polymer codoped with ETM have also been investigated.[33–35] Such devices have advantageously easy manufacturing in terms of a single spin-coating process.[30–35] Based on the above, the incorporation of ETM or HTM shows dramatic improvement of EL performance of PLEDs. Nevertheless, EL improvement of polymer blend-based devices through electron and hole flux balance has not been thoroughly examined.[30–35] Studying the current characteristics of polymer blend-based hole-only and electron-only devices helps in understanding the charge transporting material blending effect on EL properties.[36–38] Apart from that, EL performances of polymer blend-based devices are also affected by compatibility between the LEP and charge transporting material. Thin film morphology effect on EL properties has not to our knowledge been discussed in detail for such polymer blend-based devices.[30–35]

We have recently synthesized a novel triarylaminooxadiazole-containing tetraphenylsilane light-emitting polymer (PTOA).[39] The PTOA-based PLED moderate brightness and efficiency is due to EL quenching of electromer or electroplex effects. Electromer and electroplex are suppressed completely by incorporating poly(*n*-vinylcarbazole) (PVK) in PTOA film. The EL performance of the PTOA-based PLED is improved. However, PLEDs based on PTOA and PVK-PTOA light emitting layers are not charge balanced. Hole-current density is much higher than electron-current density. The imbalance between carrier injection and transportation is unfavorable in obtaining a high current efficiency device. To further enhance EL performances, various amounts of *N*-arylbenzimidazoles trimer (TPBI) are incorporated in light emitting layers of PTOA or PTOA-PVK composite films to enhance electron current density. Moreover, the ETM TPBI is inserted between the light-emitting layer and cathode interface, which helps electron injection in the light-emitting layer from the cathode. Consequently, higher EL performances of TPBI-PVK-PTOA composite film-based devices are expected due to better electron and hole charge balance. Although the ETM TPBI has been usually incorporated into the light emitting layer of small molecules-based electroluminescent devices, PLEDs based on the blending of LEP and TPBI have not been reported.[40–46] This study investigates current characteristics of TPBI-PVK-PTOA composite solid film-based hole-only and electron-only devices to further discuss EL performances of polymer blend-based devices through balanced electron and hole fluxes. Moreover, thin film morphology of TPBI-PVK-PTOA composite solid films is investigated using AFM spectroscopy. Compatibility and morphology effects on EL performances of PLEDs are also discussed.

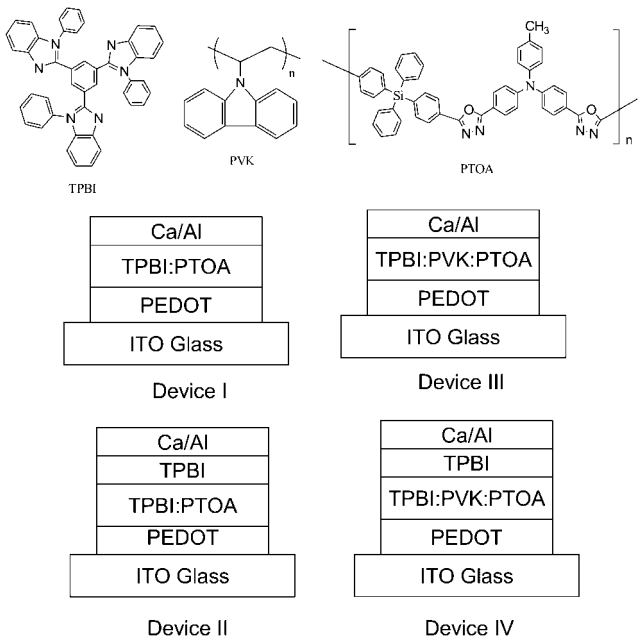

Figure 1 Chemical structure of light emitting materials and configuration of PLEDs.

EXPERIMENTAL

Chemical structures of TPBI, PVK, and PTOA are shown in Figure 1. LEP PTOA is synthesized according to the literature.[39] PVK and TPBI are purchased from Aldrich and used as received. Conjugated polymer solutions with different weight ratios of TPBI-PVK-PTOA are prepared using cyclohexanone (10 mg/mL). Compositions and sample abbreviations for LEP solutions are summarized in Table I. The UV–vis spectra of LEP composite solid films are measured using a Hewlett–Packard 8453 with a photodiode array detector. Photoluminescence and EL spectra are recorded on a Hitachi F-4500 fluorescence spectrophotometer.

PLED configurations in this study are ITO glass/PEDOT/TPBI-PTOA or TPBI-PVK-PTOA/Cathode and ITO glass/PEDOT/TPBI-PTOA/TPBI or TPBI-PVK-PTOA/TPBI/Cathode (as shown in Fig. 1). ITO-coated glass with a sheet resistance of 15 Ω/sq is purchased from Applied Film Corp. Glass substrates with patterned ITO electrodes are well washed and cleaned by O_2 plasma treatment. A thin film (60 nm) of HTM PEDOT (Baytron P AI4083, Bayer) forms on the ITO layer of a glass substrate by

TABLE I
Thin Film Thickness, Optical and Electroluminescence Properties of TPBI-PTOA Composite Films-Based Devices

Sample no.	TPBI content (wt %)	d (nm)	λ_{max}^{PL} (nm)	λ_{max}^{EL} at 18 V (nm)	FWHM of EL at 18 V (nm)	CIE (x,y) at 18 V	B (cd/m^2)	E_{ff} (cd/A)
PTOA	0	84	457	458	99	(0.20,0.26)	248	0.54
I-25	25	77	463	435	58	(0.17,0.09)	528	0.74
I-50	50	56	457	434	48	(0.16,0.06)	961	1.85
II-25	25	74	458	443	69	(0.18,0.15)	969	1.34
II-50	50	54	453	438	53	(0.16,0.08)	589	0.74

d, Thickness of light emitting layer; B, Brightness of PLED; E_{ff}, Current efficiency of PLED.

the spin-casting method. Composite films with different weight ratios (X : 70 : 30) of TPBI-PVK-PTOA are then obtained by spin-coating the 15 mg/mL cyclohexanone solution onto the PEDOT layer at a speed of 2000 rpm, and dried at 80°C for 1 h in a glove box. A TPBI electron-transporting layer (10 nm) is then deposited onto the polymer composite film. Furthermore, a high purity Ca cathode is thermally deposited onto the TPBI film, followed by Al metal deposition as the top layer in a high vacuum chamber. Moreover, the electron-only device configuration in this study is ITO glass/Ca (100 nm)/light emitting layer/Ca (15 nm)/Al (100 nm). The hole-only device configuration is ITO glass/light emitting layer/Cu (150 nm).[37,38] After electrode deposition, the PLED is transferred from the evaporation chamber to a glove box purged by high purity nitrogen gas to keep oxygen and moisture levels below 1 ppm. The device is encapsulated by glass covers, and sealed with UV-cured epoxy glue in the glove box. The cathode deposition rate is determined with a quartz thickness monitor (STM-100/MF, Sycon). Thickness of the thin film is determined with a surface texture analysis system (3030ST, Dektak). Current–voltage characteristics are measured on a programmable electrometer with current and voltage sources (Keithley 2400). Luminance is measured with a BM-9 luminance meter (Topcon).

RESULTS AND DISCUSSION

PLEDs based on the light emitting layer of TPBI-PTOA or TPBI-PVK-PTOA composite films are fabricated. The incorporating effects of electron transporting material TPBI on morphology, optical properties, and EL performances of PTOA, and PVK-PTOA-based PLEDs are discussed as follows:

Morphology and optoelectronic properties of devices I and II

AFM spectra of TPBI-PTOA composite films

The morphology and compatibility of TPBI-PTOA-based composite films are investigated using AFM microscopy. The AFM spectra of TPBI-PTOA-based composite films are shown in Figure 2. No phase separation occurred for the TPBI-PTOA-based composite films, as seen from the phase images of composite films. TPBI dispersed uniformly in the PTOA polymer matrix, even though some area protruded from the composite film surface. Despite this, average surface roughness of TPBI-PTOA-based composite films is only about 0.5 nm. Smooth surface of TPBI-PTOA film results in excellent contact between the light emitting layer and cathode. This condition is favorable for electron injection from the cathode.

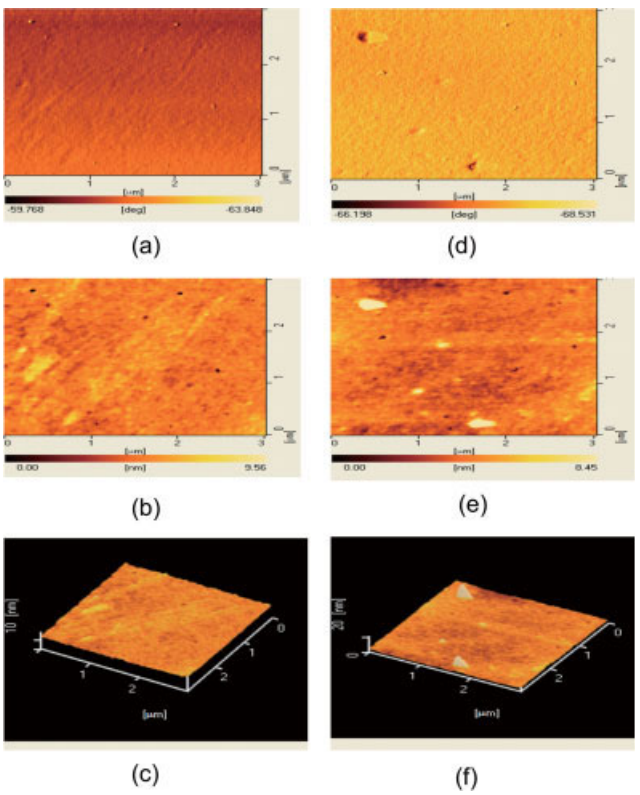

Figure 2 AFM spectra of TPBI-PTOA composite films ((a), (b), and (c): TPBI : PTOA = 25 : 75 wt %; (d), (e), and (f): TPBI : PTOA = 50/50 wt %; (a),(d): Phase image; (b),(e):Topography image; (c), (f): 3D Topography image). [Color figure can be viewed in the online issue, which is available at www.interscience.wiley.com.]

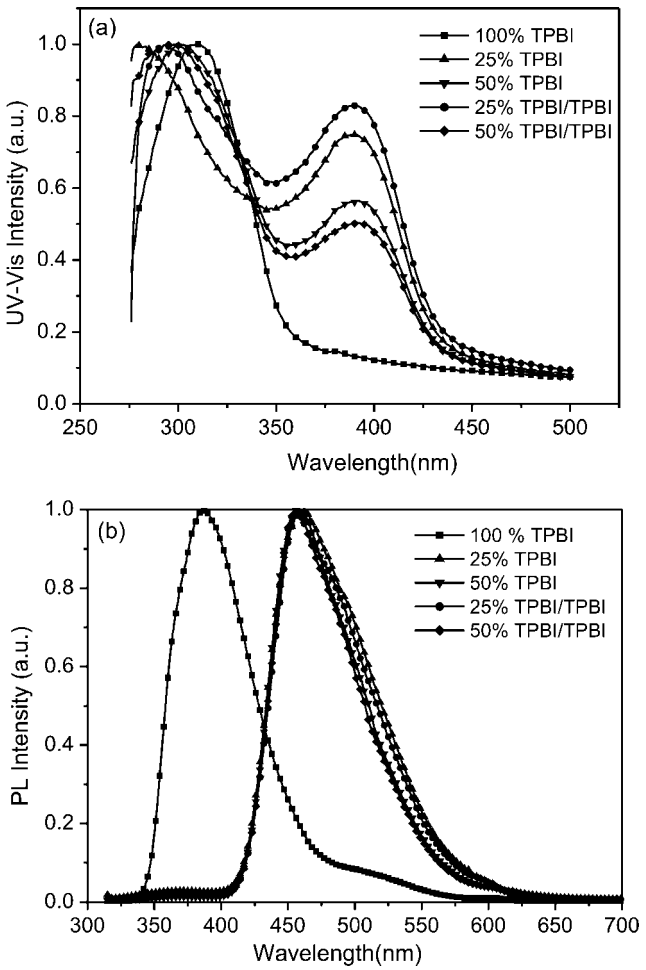

Figure 3 UV–vis and PL spectra of TPBI-PTOA and TPBI-PTOA/TPBI (10 nm)-based composite films (exciting wavelength: 300 nm).

UV–vis absorption and PL spectra of TPBI-PTOA composite films

Figure 3 shows the UV–vis absorption and PL spectra of TPBI-PTOA and TPBI-PTOA/TPBI composite films. The composition, film thickness, and maximum wavelength emission of PL (λ_{max}^{PL}) for the TPBI-PTOA and TPBI-PTOA/TPBI composite films are summarized in Table I. The TPBI-PTOA composite films have an absorption band with a maximum at 380 nm, and an absorption band range from 275 to 350 nm. The absorption band with a 380-nm maximum attributes to the π conjugation between diphenyl(*para*-tolyl)amine and the oxadiazole unit of PTOA.[39] Absorption intensity decreases with increasing TPBI content, while maximal absorption position is concentration-independent for the PTOA. Conversely, the TPBI absorption peak positions strongly depend on TPBI concentration in TPBI-PTOA composite film and vary from 305 to 275 nm. This blue shift phenomenon is the same as TPBI solvatochromic effect in solution state.[41] Moreover, the same absorption behaviors are observed for TPBI-PTOA/TPBI bi-layer composite films. TPBI also shows PL with maximum emission at around 375 nm. The PL emission of TPBI absorbs completely by the triarylaminooxdiazole of PTOA via the Forster-type energy transfer process for TPBI-PTOA composite films. As a result, maximum PL emission is observed at 460 nm, attributed to the triarylaminooxdiazole group light-emitting unit.[39] The full width at half-maximum (FWHM) PL emission band also reduces with increasing TPBI content for TPBI-PTOA composite films. This result attributes to excimer formation suppression between PTOA polymer chain segments.[39] The same PL spectra are also observed for composite films based on the TPBI-PTOA/TPBI bi-layer.

EL spectra of devices I and II

EL spectra of PLEDs with a single layer of TPBI-PTOA (devices I-25 and I-50) and bi-layer of TPBI-PTOA/TPBI (devices II-25 and II-50) composite films as a light-emitting layer at various applied voltages are shown in Figures 4 and 5, respectively. Maximum emission wavelength of EL (λ_{max}^{EL}), FWHM of EL, and Commission Internationale de L'Eclairage ($CIE_{x,y}$) coordinates for the TPBI-PTOA and TPBI-PTOA/TPBI-based devices are summarized in Table I. Two emission peaks with maximum at around 410 and 458 nm are observed at low applied voltage (12V) for devices I-25 and I-50. The emission band with a maximum at 410-nm attributes to TPBI light emission.[40] PTOA shows maximum emission at around 458 nm.[39] The EL spectra vary with increasing applied voltages. Increasing applied voltage to 18 V, suppresses the TPBI and PTOA emission peaks. A new emission peak located at about the 435-nm wavelength is observed. The emission peak at about the 435-nm wavelength possibly attributes to electrical field-induced electroplex formation between the electron acceptor TPBI and electron–donor moiety of PTOA.[39] Moreover, the emission peak may attribute to the blue shift of the PTOA emission peak, originally showing up at 458 nm. The PTOA EL emission blue shifting for about 23 nm, attributes to the thermochromism phenomenon as the device driving with high current density.[47] Heeger and coworkers report a similar phenomenon in the MEH-PPV-based device.[47] However, we could not confirm that the emission peak at around 435 nm is only attributed to PTOA emitting. The TPBI emission intensity generally increases with increasing applied voltage. Moreover, the TPBI emission peak slightly shifts to a longer wavelength with increasing applied voltage. Consequently, the emission peak at 435-nm

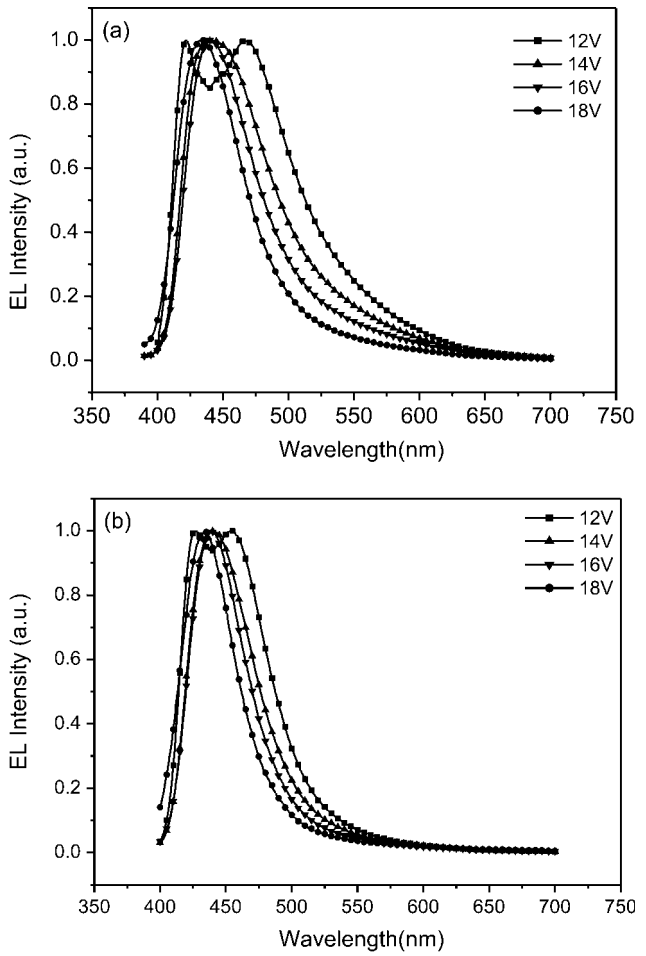

Figure 4 EL spectra of TPBI-PTOA composite films-based devices under various applied voltages ((a) TPBI-PTOA = 25 : 75(Device I-25), and (b) TPBI-PTOA = 50 : 50 (Device I-50)).

attributes to electroplex emission of TPBI and PTOA or the thermochromism of PTOA. Device I-50 has the same EL spectrum as device I-25. In Table I, the FWHM of PTOA emission band becomes resoundingly narrower, and color purity enhances with increasing TPBI content for the TPBI-PTOA composite film-based devices. High TPBI content also leads to enhanced suppression of electromer or electroplex formation between the diphenyl(4-tolyl)amine and oxadiazole groups of PTOA.[39] On the other hand, TPBI and PTOA emission peaks with maximum at around 410 and 458 nm are observed at the applied voltage range from 12 to 16 V for device II-25, as shown in Figure 5. Only one emission peak is observed at wavelength of 443 nm with increasing applied voltage of 18 V, attributed to the electroplex emission of TPBI and PTOA or the thermochromism of PTOA. Electroplex is observed at a higher applied voltage for device II-25 compared with device I-25. This result is due to TPBI layer insertion between the light emitting layer and the cathode. EL spectra depend on ETL presence. Charge recombination zone shifting is proposed for EL spectra variation. Electroplex formation, between the PTOA and TPBI varies with applied voltage.[48] The same EL spectra are observed for device II-50. In Table I, the FWHM of PTOA emission band becomes narrower, and color purity enhanced with increasing TPBI content for devices II-25 and II-50. Electromer or electroplex suppression is indeed enhanced with increasing TPBI content.

Current density, brightness, and current efficiency of devices I and II

The EL properties of TPBI-PTOA (devices I-25 and I-50) and TPBI-PTOA/TPBI (devices II-25 and II-50)-based devices are shown in Figure 6. Maximal brightness and current efficiency are summarized in Table I. Lower turn-on voltage, higher brightness, and larger current efficiency are obtained for the TPBI-PTOA and TPBI-PTOA/TPBI composite film-based devices compared with the pure PTOA-based device. The presence of ETM TPBI in PTOA film results in enhanced electron-transporting capacity of the light-emitting layer. A better charge balance of electron and hole is obtained. Therefore, brightness and current efficiency increase with increasing TPBI content for devices I-25 and I-50. Moreover, TPBI layer insertion enhances electron-injection in the light emitting layer. This is also favorable for electron and hole charge balance. As a result, device II-25 brightness and efficiency is better than device I-25. Reducing light emitting layer thickness with increasing TPBI concentration is another reason for TPBI-PTOA-based devices with higher brightness and larger current efficiency than the one based on PTOA. EL performances are also dependent on light

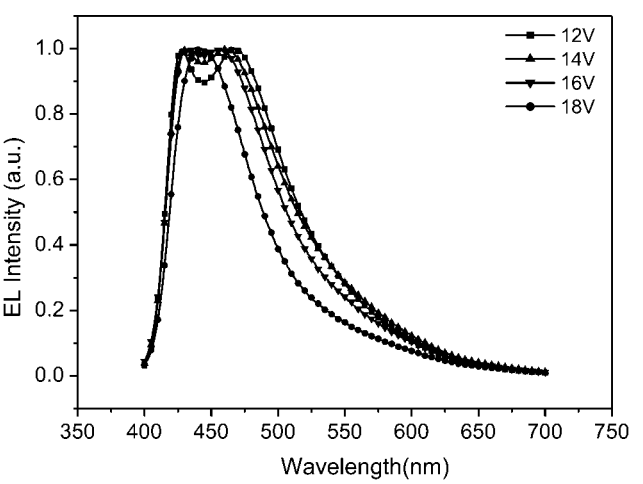

Figure 5 EL spectra of TPBI-PTOA (25 : 75)/TPBI (10 nm) composite film-based device (Device II-25) under various applied voltages.

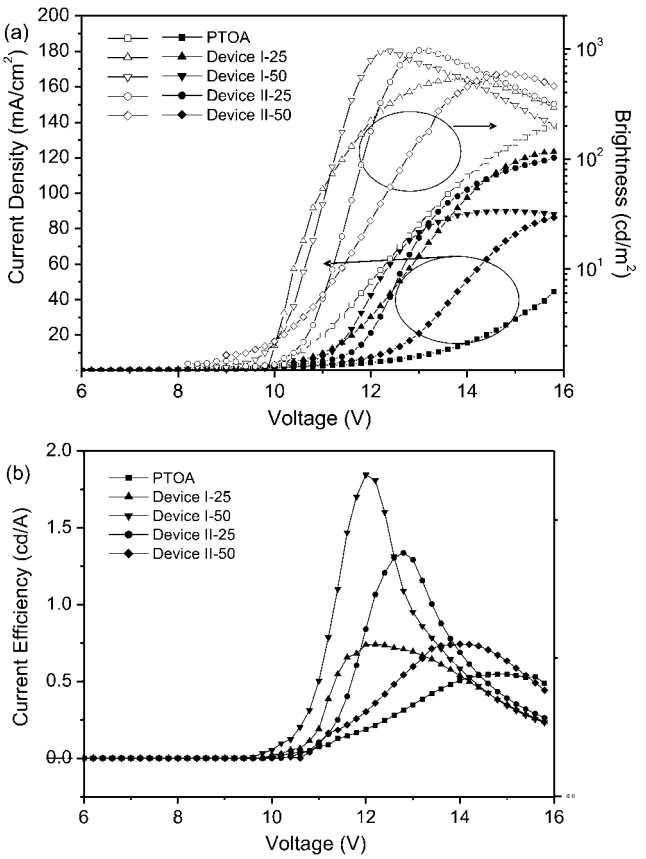

Figure 6 Current density, brightness, and current efficiency versus applied voltage for devices I and II with various TPBI contents.

emitting layer thickness.[12] However, the brightness and efficiency of device II-50 is not better than device II-25. This is possibly due to unbalanced electron and hole for device II-50. Device II-50 with excess TPBI content was not favorable for the charge balance of electron and hole, leading to reduced current efficiency. Apart from that, Device II-50 with lower current efficiency is attributed to its thinner light emitting layer thickness, compared with that of Device II-25. Particle presence on the ITO glass surface and ITO surface roughness, cannot be smoothed down by a thin polymer film. As a result, electric leakage could have occurred during PLED operation processes because of defect presence. Consequently, low brightness and current efficiency are obtained for the PLED with a thin light emitting layer thickness.

Current densities of TPBI-PTOA composite film based on electron-only and hole-only devices

Electron-only and hole-only devices with various light emitting TPBI-PTOA and TPBI-PTOA/TPBI composite film layers are fabricated to understand TPBI influence on electron injection and transportation in TPBI-PTOA composite film-based devices. Energy level diagrams of the electron-only and hole-only devices with various light emitting TPBI-PTOA and TPBI-PTOA/TPBI composite film layers are shown in Figure 7. Current densities of electron-only and hole-only devices are shown in Figure 8. For electron-only devices, electron-current density increases with increasing TPBI content for TPBI-PTOA composite film-based devices because of TPBI electron-withdrawing property. As shown in Figure 7(a), the lowest unoccupied molecular orbital (LUMO) levels of PTOA and TPBI are 2.45 and 2.7 eV, respectively. TPBI incorporation is helpful for electron-injection into the TPBI-PTOA film from the cathode layer. Moreover, TPBI-PTOA/TPBI-based devices show higher current density than those based on TPBI-PTOA. This is due to TPBI with a lower LUMO level than the PTOA. However, reduced thin film thickness is another reason for enhanced electron–current density, especially for the TPBI-PTOA film containing 50 wt % of TPBI under highly applied voltages. On the other hand, hole-current density reduces for the TPBI-PTOA-based device compared with the PTOA-based device. The highest occupied molecular orbital (HOMO) levels of PTOA and TPBI are 5.3 and 6.2 eV, respectively. TPBI plays a hole-trapper role in the light-emitting layer. Never-

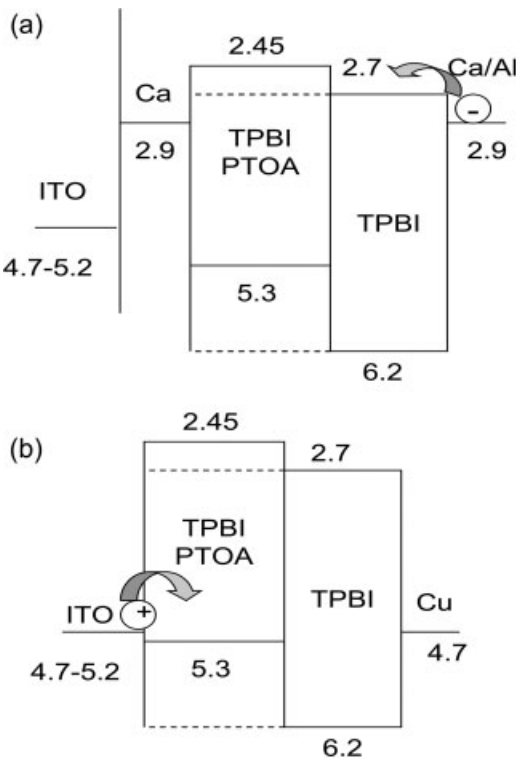

Figure 7 Energy level diagrams of the (a) electron-only and (b) hole-only devices based on single layer and bilayer of TPBI-PTOA and TPBI-PTOA/TPBI (10 nm), respectively.

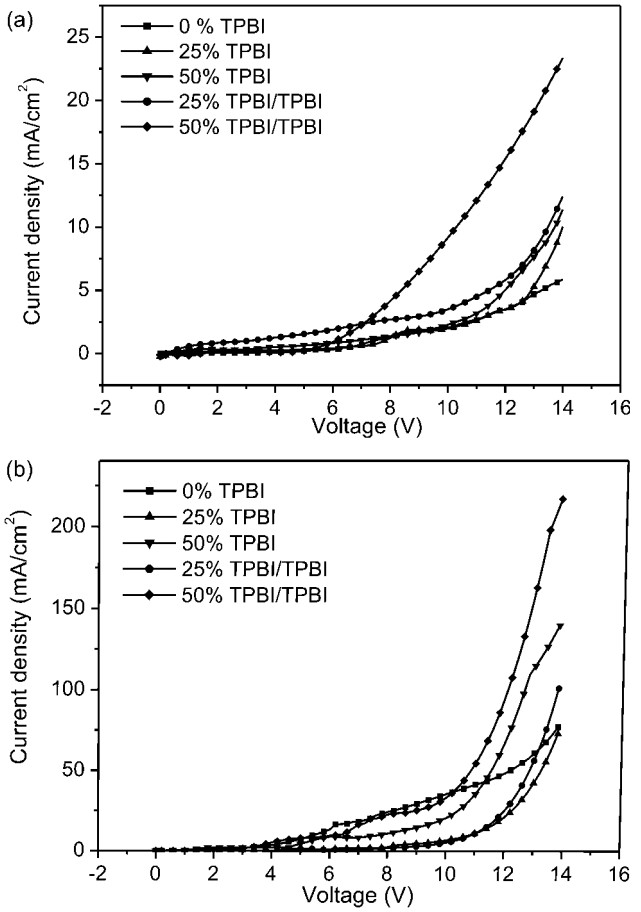

Figure 8 Current densities versus applied voltage for the (a) electron-only and (b) hole-only devices based on single layer and bilayer of TPBI-PTOA and TPBI-PTOA/TPBI (10 nm), respectively.

theless, reduced thin film thickness results in enhanced hole-current density for the TPBI-PTOA film containing 50 wt % of TPBI under highly applied voltages. As a result, the hole-only device containing 50 wt % TPBI shows a higher hole-current density than the one containing 25 wt % of TPBI.

Morphology and optoelectronic properties of devices III and IV

AFM and PL spectra of TPBI-PVK-PTOA-based composite films

Composition and film thickness of the TPBI-PVK-PTOA and TPBI-PVK-PTOA/TPBI composite films are summarized in Table II. Surface morphology and compatibility of the TPBI-PVK-PTOA composite solid films are investigated using AFM microscopy. AFM spectra of TPBI-PVK-PTOA composite films are shown in Figure 9. From AFM phase images, one enclosed phase and one continuous phase are observed for composite films. The dark region is an enclosed phase, corresponding to the thinner composite solid film area. The bright continuous phase region is attributed to thin film surface protrusion. This is due to poor compatibility between the TPBI and PVK-PTOA matrix, since PVK and PTOA have excellent compatibility in solid film.[39] As a result, TPBI separates from the PVK-PTOA polymer matrix.

PL spectra of TPBI-PVK-PTOA composite films are shown in Figure 10. Emission peak from maximum PTOA at 451 nm is observed for composite films containing various TPBI contents. PL spectra are independent of TPBI concentration. No PL emission peak from TPBI is observed at 410 nm. Despite that TPBI is nano-phase separated from the PVK-PTOA polymer matrix, PL emissions from TPBI and PVK are completely absorbed by PTOA via the Forster-type energy transfer process. The same PL spectra are observed for composite films based on the TPBI-PVK-PTOA/TPBI bi-layer.

EL spectra of devices III and IV

EL spectra of TPBI-PVK-PTOA and TPBI-PVK-PTOA/TPBI composite film-based devices III and IV are shown in Figure 11. Maximum emission wavelength of EL, FWHM of EL, and CIE coordinates for devices III and IV are summarized in Table II. Maximum emission wavelength and FWHM of EL for

TABLE II
Thin Film Thickness, Optical and Electroluminescence Properties of TPBI-PVK-PTOA (X:70 : 30 wt.%) Composite Films-Based Devices

Sample no.	TPBI content X (wt %)	d (nm)	λ_{max}^{PL} (nm)	λ_{max}^{EL} at 12 V (nm)	FWHM of EL at 12 V (nm)	CIE (x,y) at 12 V	B (cd/m^2)	E_{ff} (cd/A)
III-0	0	81.0	451	439	57	(0.16,0.10)	503	0.41
III-5	5	79.2	451	441	50	(0.16,0.13)	263	0.23
III-15	15	68.8	451	441	49	(0.17,0.11)	215	0.22
III-30	25	62.8	451	440	48	(0.16,0.10)	148	0.12
IV-0	0	81.0	449	442	50	(0.15,0.09)	342	0.22
IV-5	5	77.6	450	443	50	(0.16,0.10)	188	0.15
IV-15	15	69.2	451	444	51	(0.16,0.11)	149	0.10
IV-30	25	63.6	450	442	51	(0.16,0.10)	50	0.09

d, Thickness of light emitting layer; B, Brightness of PLED; E_{ff}, Current efficiency of PLED.

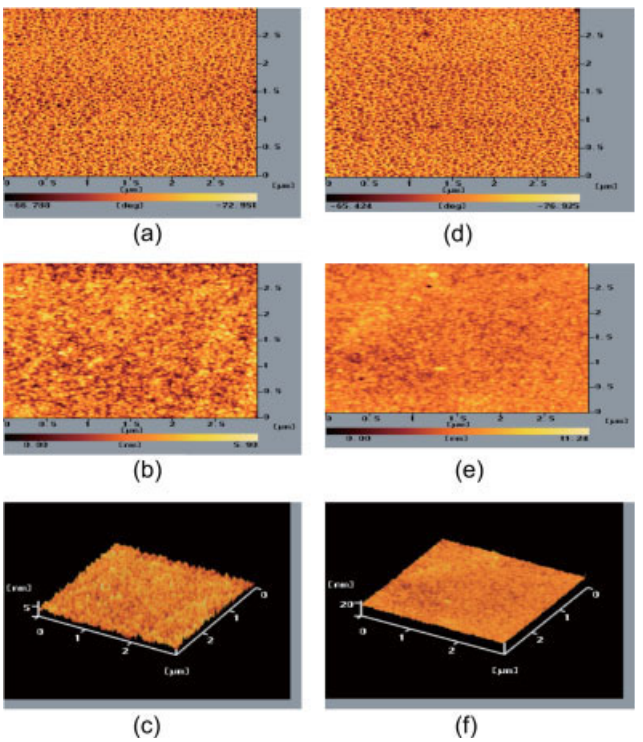

Figure 9 AFM spectra of TPBI-PVK-PTOA (X: 70 : 30 wt %) composite films ((a), (b), and (c): $X = 15$; (d), (e), and (f): $X = 25$; (a), (d): Phase image; (b), (e): Topography image; (c), (f): 3D Topography image). [Color figure can be viewed in the online issue, which is available at www.interscience.wiley.com.]

device III are not changed significantly with TPBI incorporation in the PVK-PTOA composite film-based light emitting layer. Therefore, blue emission color purities are not enhanced as compared to the device based on PVK-PTOA (device III-0). Moreover, the EL emission band changes only slightly with increasing TPBI content. This is due to TPBI separation from the PVK-PTOA polymer matrix. Poor compatibility results in little TPBI influence on the EL spectra of the composite film based device. The same result is observed for device IV compared to device III-0. Color purities do not improve with TPBI layer insertion in the light-emitting layer and cathode interface. EL spectra of device IV-15 under various applied voltages is shown in Figure 12. EL emission bands of TPBI-PVK-PTOA composite film-based devices are voltage-independent. The same result is observed for devices III and IV containing various TPBI contents.

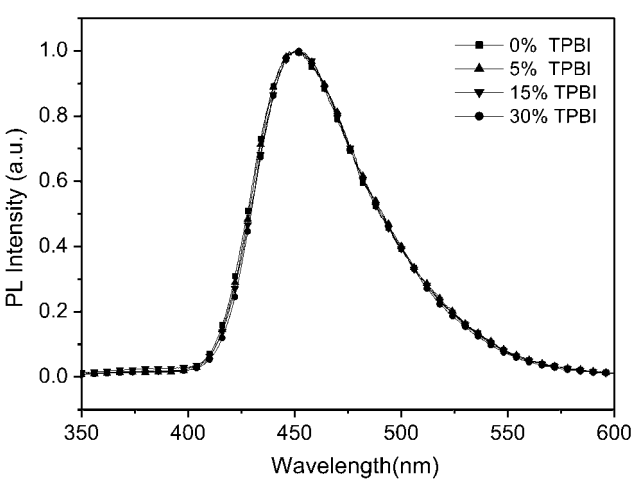

Figure 10 PL spectra of TPBI-PVK-PTOA (X : 70 : 30 wt %) composite films (exciting wavelength: 300 nm).

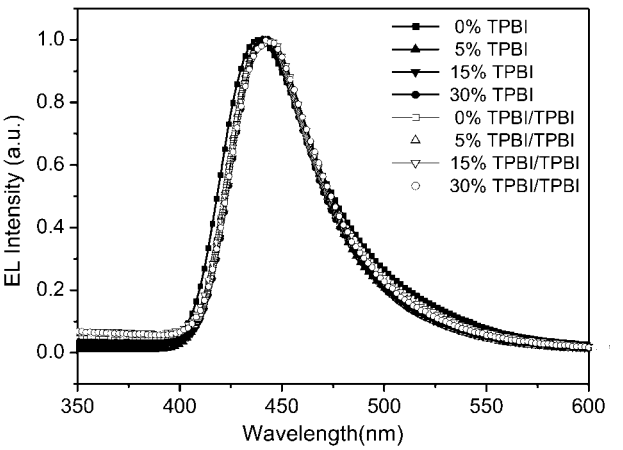

Figure 11 EL spectra of TPBI-PVK-PTOA (X : 70 : 30 wt %) and TPBI-PVK-PTOA (X : 70 : 30 wt %)/TPBI (10 nm) composite films-based PLEDs under applied voltage of 12 V.

Current density, brightness, and power efficiency of devices III and IV

EL properties versus applied voltage of TPBI-PVK-PTOA composite film-based devices III and IV are shown in Figure 13. Maximum brightness and current efficiency for devices III and IV are summar-

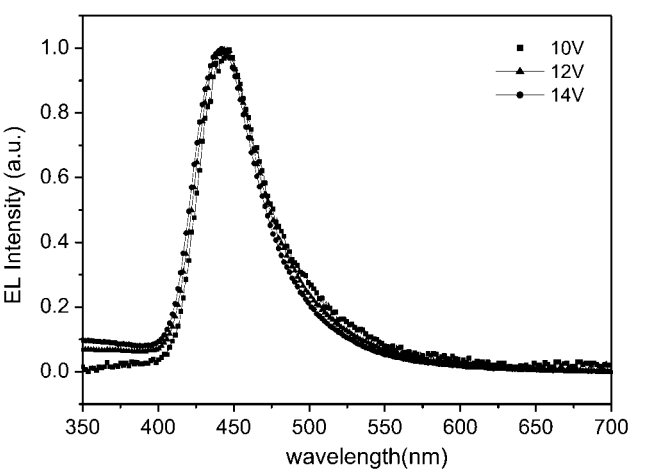

Figure 12 EL spectra of TPBI-PVK-PTOA (15 : 70 : 30 wt %)/TPBI (10 nm) composite film-based device (IV-15) under various applied voltages.

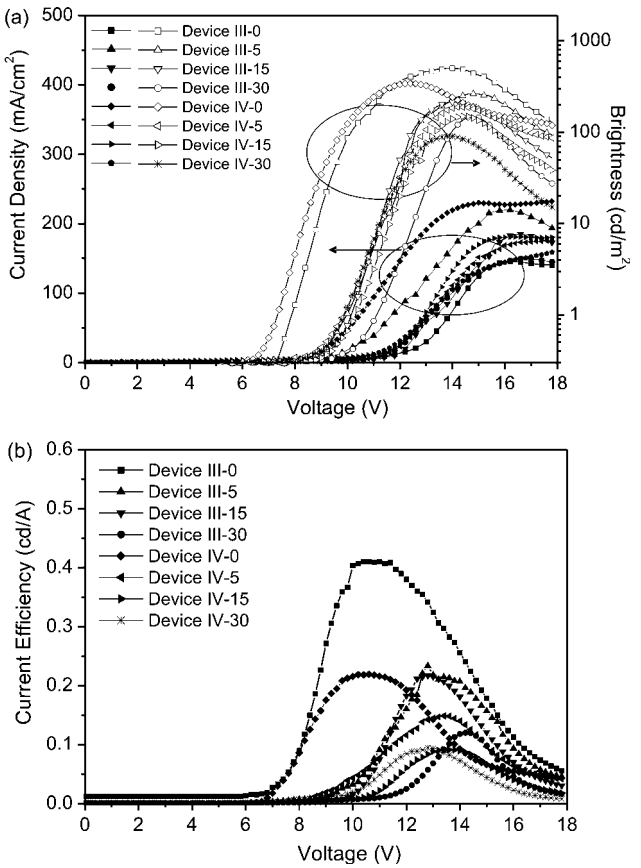

Figure 13 Current density, brightness, and current efficiency versus applied voltage for devices III and IV with various TPBI contents.

ized in Table II. In Figure 13, brightness and current efficiency reduce with increasing TPBI content for device III. Brightness and current efficiency do not enhance as expected by incorporating ETM TPBI in the light-emitting layer. Reducing light emitting layer thickness is not favorable for EL performance enhancement. Moreover, turn on voltage increases with increasing TPBI content. In addition to the unbalanced electron and hole, reduced blue emitter PTOA content and poor compatibility between TPBI and PVK-PTOA in the light emitting layer lead to reduced EL performances of device III. The separation of TPBI from PTOA-PVK composite film is evidenced by AFM images, shown in Figure 8. Consequently, EL performances of device III are not enhanced with incorporating TPBI as well as devices I and II. The same result is observed for device IV. Furthermore, brightness and current efficiency reduce for device IV compared to device III. EL performances do not improve with TPBI electron transporting layer insertion in the light-emitting layer and cathode interface. A poor combination between the TPBI electron-transporting layer and the TPBI-PVK-PTOA layer causes further reduced EL performances.

Current densities of TPBI-PVK-PTOA composite film based on electron-only and hole-only devices

To understand TPBI influence on electron injection and transportation in TPBI-PVK-PTOA composite film-based devices, electron-only and hole-only devices containing various light emitting layers of TPBI-PVK-PTOA composite films are fabricated. Energy level diagrams of electron-only and hole-only devices containing various light emitting layers of TPBI-PVK-PTOA composite films are shown in Figure 14. Current densities of electron-only and hole-only devices containing various light emitting layers are shown in Figure 15. For the PTOA-based device, hole-current density is larger than electron-current density. Electron-current density reduces significantly, while hole-current density enhances slightly as PTOA blends with PVK. This is because PVK (2.2 eV) has a higher LUMO level than PTOA (2.45 eV), as shown in Figure 14(a). PVK incorporation is not helpful for electron-injection into the TPBI-PVK-PTOA film from the cathode layer. Electron and hole current densities indicate that the hole is the major carrier for the device based on the light-emitting layer of PTOA-PVK composite film, as well as the one based on PTOA film only. As ETM TPBI incorporates into PVK-PTOA composite film or is inserted in the light-emitting layer and cathode interface, electron current density magnitude enhances and achieves the same order

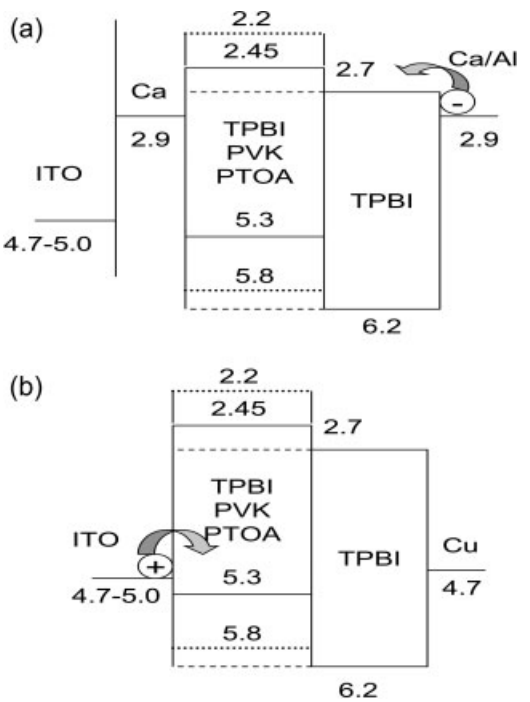

Figure 14 Energy level diagrams of the (a) electron-only and (b) hole-only devices with different TPBI-PVK-PTOA composite films-based light emitting layers, respectively.

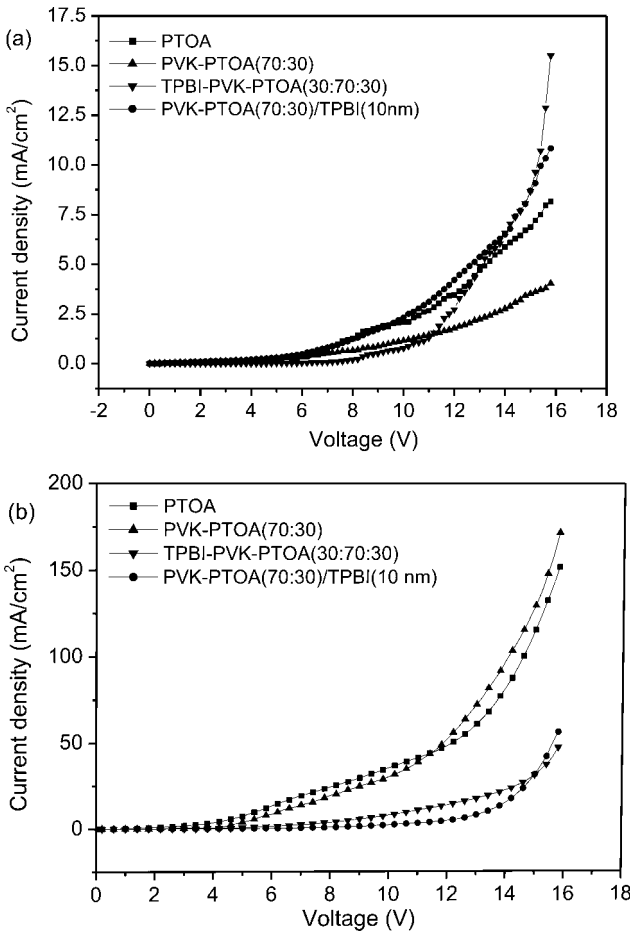

Figure 15 Current densities of electron-only and hole-only devices with different TPBI-PVK-PTOA composite films-based light emitting layers.

compared with the device based on PTOA only. Low LUMO level of TPBI (2.7 eV) is favorable for electron-injection into TPBI-PVK-PTOA film from the cathode layer. Conversely, hole-current density reduces significantly compared with the devices based on the light-emitting layer of PTOA or PTOA-PVK composite films. This is due to TPBI as a hole-trapper in the light-emitting layer. TPBI (6.2 eV) shows a lower HOMO level than that of PTOA (5.3 eV) and PVK (5.8 eV). However, hole current density reduction is not favorable for recombining electron and hole in the light-emitting layer, even though electron current density slightly enhances. Therefore, brightness and current efficiency do not enhance with TPBI incorporation in PVK-PTOA composite film-based devices.

CONCLUSIONS

Doping TPBI electron-transporting material in the light emitting layer enhances EL performances of PTOA-based blue light emitting device because of enhanced charge balance and suppressed excimer formation between polymer chains. In addition to electron and hole charge balance, polymer blend compatibility is an important issue for enhanced EL performances of composite film-based PLED. EL performances reduce with TPBI doped in PVK-PTOA-based devices due to poor compatibility between TPBI and PVK. EL performances are also determined by the amount of electron-injection in the light-emitting layer. Inserting the TPBI layer in the light emitting layer and cathode interface enhances EL performances of TPBI-PTOA-based devices, while the TPBI-PVK-PTOA device reduces due to poor contact between the TPBI-PVK-PTOA light emitting layer and TPBI electron transporting layer.

References

1. Kobayashi, H.; Kanbe, S.; Seki, S.; Kigchi, H.; Kimura, M.; Yudasaka, I.; Miyashita, S.; Shimoda, T.; Towns, C. R.; Burroughes, J. H.; Friend, R. H. Synth Met 2000, 111/112, 125.
2. Vaart, N. C. V. D.; Lifka, H.; Budzelaar, F. P. M.; Rubingh, J. E. J. M.; Hoppenbrouwers, J. J. L.; Dijksman, J. F.; Verbeek, R. G. F. A.; Woudenberg, R. V.; Vossen, F. J.; Hiddink, M. G. H.; Rosink, J. J. W. M.; Bernards, T. N. M.; Giraldo, A.; Young, N. D.; Fish, D. A.; Childs, M. J.; Steer, W. A.; Lee, D.; George, D. S. SID Symp 2004, 35, 1284.
3. Millard, I. S. Synth Met 2000, 111/112, 119.
4. Bernius, M.; Inbasekaran, M.; Woo, E.; Wu, W.; Wujkowski, L. Thin Solid Film 2000, 363, 55.
5. Kim, J. S.; Granstrom, M.; Friend, R. H.; Johansson, N.; Salaneck, W. R.; Daik, R.; Feast, W. J.; Calcialli, F. J Appl Phys 1998, 84, 6859.
6. Kim, J. S.; Friend, R. H.; Cacialli, F. Appl Phys Lett 1999, 74, 3084.
7. Kim, J. S.; Cacialli, F.; Cola, A.; Gigli, G.; Cingolani, R. Appl Phys Lett 1999, 75, 19.
8. Low, B.; Zhu, F.; Zhang, K.; Chua, S. Appl Phys Lett 2002, 80, 4659.
9. Liu, J.; Shi, Y.; Ma, L.; Yang, Y. J Appl Phys 2000, 88, 605.
10. Shi, Y.; Liu, J.; Yang, Y. J Appl Phys 2000, 87, 4254.
11. Liu, J.; Guo, T. F.; Shi, Y.; Yang, Y. J Appl Phys 2001, 89, 3668.
12. Lee, R. H.; Lee, Y. Z.; Chao, C. I. J Appl Polym Sci 2006, 100, 133.
13. Greczynski, G.; Fahlman, M.; Salaneck, W. R. J Chem Phys 2000, 113, 2407.
14. Brown, T. M.; Millard, I. S.; Lacey, D. J.; Burroughes, J. H; Friend, R. H.; Cacialli, F. Synth Met 2001, 124, 15.
15. Yang, X.; Mo, Y.; Yang, W.; Yu, G.; Cao, Y. Appl Phys Lett 2001, 79, 563.
16. Brown, T. M.; Lacey, D. J.; Burroughs, J. H.; Cacialli, F. Appl Phys Lett 2000, 77, 3096.
17. Karg, S.; Scoot, J. C.; Salem, J. R.; Angelopoulos, M. Synth Met 1996, 80, 111.
18. Lee, K. Y.; Kim, Y. K.; Kwon, O. K.; Lee, J. W.; Shin, D. M.; Kim, D. Y.; Sohn, B. C.; Choi, D. S. Thin Solid Film 2000, 363, 225.
19. Elschner, A.; Bruder, F.; Heuer, H. W.; Jonas, F.; Karbach, A.; Kirchmeyer, S.; Thurm, S.; Wehrmann, R. Synth Met 2000, 111/112, 139.
20. Obrien, D.; Bleyer, A.; Lidzey, D. G.; Bradley, D. D. C.; Tsutsui, T. J Appl Phys 1997, 82, 2662.
21. Geng, Y.; Chen, A. C. A.; Qu, J. J.; Chen, S. H; Klubek, K.; Vaeth, K. M.; Tang, C. W. Chem Mater 2003, 15, 4352.

22. Chen, Z. K.; Meng, H.; Lai, Y. H.; Huang, W. Macromolecules 1999, 32, 4351.
23. Chung, S. J.; Kwon, K. Y.; Lee, S. W.; Jin, J. I.; Lee, C. H.; Lee, C. H.; Park, Y. Adv Mater 1998, 10, 1112.
24. Lee, N. H. S.; Chen, Z. K.; Chua, S. J.; Lai, Y. H.; Huang, W. Thin Solid Film 2000, 363, 106.
25. Wu, F. I.; Reddy, D. S.; Shu, C. F. Chem Mater 2003, 15, 269.
26. Kim, J. H.; Lee, H. Synth Met 2004, 144, 169.
27. Chen, S. H.; Chen, Y. Macromolecules 2005, 38, 53.
28. Ha, J.; Vacha, M.; Khanchaitit, P.; Ong, D. A.; Lee, S. H.; Ogio, K.; Sato, H. Synth Met 2004, 144, 151.
29. Liao, L.; Pang, Y.; Ding, L.; Karasz, F. E. Macromolecules 2004, 37, 3970.
30. Suh, M. C.; Chin, B. D.; Kim, M. H.; Kang, T. M.; Lee, S. T. Adv Mater 2003, 15, 1254.
31. Cea, P.; Hua, Y.; Pearson, C.; Wang, C.; Bryce, M. R.; Royo, F. M.; Petty, M. C. Thin Solid Film 2002, 408, 275.
32. Ahn, J. H.; Wang, C.; Pearson, C.; Bryce, M. R.; Petty, M. C. Appl Phys Lett 2004, 85, 1283.
33. Gong, X.; Ostrowski, J. C.; Moses, D.; Bazan, G. C.; Heeger, A. J Adv Funct Mater 2003, 13, 439.
34. Yang, X. H.; Neher, D. Appl Phys Lett 2004, 84, 2476.
35. Nakamura, A.; Tada, T.; Mizukami, M.; Yagyu, S. Appl Phys Lett 2004, 84, 130.
36. Lee, R. H.; Lai, H. H. Eur Polym Mater 2007, 43, 715.
37. Heeger, A. J.; Parker, I. D.; Yang, Y. Synth Metal 1994, 67, 23.
38. Park, I. D. J Appl Phys 1994, 75, 1656.
39. Lee, R. H.; Hsu, H. F.; Chan, L. H.; Chen, C. T. Polymer 2006, 47, 7001.
40. Chen, B.; Zhang, X. H.; Lin, X. Q.; Kwong, H. L.; Wong, N. B.; Lee, C. S.; Gambling, W. A.; Lee, S. T. Synth Metal 2001, 118, 193.
41. Gao, Z. Q.; Lee, C. S.; Bello, I.; Lee, S. T.; Chen, R. M.; Luh, T. Y.; Shi, J.; Tang, C. W. Appl Phys Lett 1999, 74, 865.
42. Tao, Y. T.; Balasubramaniam, E.; Danel, A.; Tomasik, P. Appl Phys Lett 2000, 77, 933.
43. Balasubramaniam, E.; Tao, Y. T.; Danel, A.; Tomasik, P. Chem Mater 2000, 12, 2788.
44. Gao, Z. Q.; Lee, C. S.; Bello, I.; Lee, S. T.; Wu, S. K.; Yan, Z. L.; Zhang, X. H. Synth Metal 1999, 105, 141.
45. Thomas, K. R. J.; Lin, J. T.; Tao, Y. T.; Chuen, C. H. Chem Mater 2004, 16, 5437.
46. Gebeyehu, D.; Walzer, K.; He, G.; Pfeiffer, M.; Leo, K.; Brandt, J.; Gerhard, A.; Stobel, P.; Vestweber, H. Synth Metal 2005, 148, 205.
47. Braun, D.; Moses, D.; Zhang, C.; Heeger, A. J Appl Phys Lett 1992, 61, 3092.
48. Chan, L. H.; Lee, R. H.; Hsieh, C. F.; Yeh, H. C.; Chen, C. T. 2002, 124, 6469.